Virology 526 (2019) 105–116

Contents lists available at ScienceDirect

Virology

journal homepage: www.elsevier.com/locate/virology

Screening and evaluation of antiviral compounds against Equid alpha-herpesviruses using an impedance-based cellular assay

Côme J. Thieulent[a,b,1], Erika S. Hue[a,b,c,1], Christine I. Fortier[a,b,c], Patrick Dallemagne[d], Stéphan Zientara[e], Hélène Munier-Lehmann[f], Aymeric Hans[g], Guillaume D. Fortier[a,b], Pierre-Hugues Pitel[a], Pierre-Olivier Vidalain[h], Stéphane L. Pronost[a,b,c,*]

[a] LABÉO Frank Duncombe, 14280 Saint-Contest, France
[b] Normandie Univ, UNICAEN, BIOTARGEN EA7450, 14280 Saint-Contest, France
[c] Normandie Univ, UNICAEN, ImpedanCELL core facility, SF 4206 ICORE, 14280 Saint-Contest, France
[d] Normandie Univ, UNICAEN, CERMN EA4258, 14000 Caen, France
[e] Université Paris-Est, Laboratoire de Santé Animale, ANSES, INRA, ENVA, UMR 1161 Virologie, 94700 Maisons-Alfort, France
[f] Institut Pasteur, Unité de Chimie et Biocatalyse, CNRS UMR 3523, 75015 Paris, France
[g] ANSES, Laboratoire de pathologie équine de Dozulé, Unité de virologie et parasitologie équine, 14430 Dozulé, France
[h] Equipe Chimie et Biologie, Modélisation et Immunologie pour la Thérapie (CBMIT), Université Paris Descartes, CNRS UMR 8601, 75006 Paris, France

ARTICLE INFO

Keywords:
Aciclovir
Antiviral
Equid herpesviruses
Ganciclovir
Impedance
Real-time cell analysis
Screening
Spironolactone
xCELLigence

ABSTRACT

Equid alpha-herpesviruses (EHV) are responsible for different diseases in equine population. EHV-1 causes respiratory diseases, abortions and nervous disorders, EHV-4 causes respiratory diseases and sporadic abortion, while EHV-3 is responsible of equine coital exanthema. In view of the lack of efficacy of vaccines against EHV-1 and EHV-4 and in the absence of vaccines against EHV-3, the use of antiviral treatment is of great interest. In this study, we documented the interest of the Real-Time Cell Analysis (RTCA) technology to monitor the cytopathic effects induced by these viruses on equine dermal cells, and established the efficacy of this method to evaluate the antiviral effect of aciclovir (ACV) and ganciclovir (GCV). In addition, the RTCA technology has also been found appropriate for the high-throughput screening of small molecules against EHV, allowing the identification of spironolactone as a novel antiviral against EHV.

1. Introduction

Herpesviruses (order *Herpesvirales*, family *Herpesviridae*) are enveloped viruses with a linear, double-stranded DNA genome of 125-290 kb. Five herpesviruses have been reported to infect horses, named equid herpesviruses (EHV)-1 to 5. While EHV-2 and 5 are classified as *Gammaherpesvirinae*, EHV-1, -3, and -4 belong to the *Alphaherpesvirinae* subfamily (Davison et al., 2009). EHV-1 is the most pathogenic and is endemic worldwide (Lunn et al., 2009). After the initial replication phase that takes place in the respiratory epithelium and draining lymph nodes, EHV-1 spreads to other organs during the cell-associated viraemia and may induce secondary forms of disease (Paillot et al., 2008). EHV-1 is a major cause of abortion in mares due to infection of endometrial endothelial cells and fetuses (Léon et al., 2008). Besides, EHV-1 can also reach the central nervous system, infect endothelial cells, and cause equine herpesvirus myeloencephalopathy (Pusterla and Hussey, 2014). Clinical signs of neurologic dysfunction are ranging from a mild ataxia of one limb to a total paralysis, often requiring euthanasia and outbreaks of EHV occur worldwide (Barbić et al., 2012; Friday et al., 2000; Goehring et al., 2006; Henninger et al., 2007; Mori et al., 2011; Pronost et al., 2012; Traub-Dargatz et al., 2013). EHV-1 strains are usually classified into abortigenic or neurologic viruses, depending of the clinical complications induced. It has been proposed that a single amino acid change in the DNA polymerase determines the outcome of the disease, but this is still discussed (Nugent et al., 2006; Pronost et al., 2010). EHV-4, also named rhinopneumonia virus, is closely related to EHV-1 but mostly causes respiratory disease and only sporadic abortion and neonatal infection in horses (Patel and Heldens, 2005). EHV-3 is distinct from previous viruses and is responsible for equine coital exanthema, characterised by the formation of papules, pustules, ulcers and vesicles on the external genitalia of horses (Barrandeguy and Thiry, 2012). Finally, EHVs often persist and induce

* Correspondence to: LABÉO Frank Duncombe, 1 route de Rosel, 14280 Saint-Contest, France.
E-mail address: stephane.pronost@laboratoire-labeo.fr (S.L. Pronost).
[1] These authors contributed equally to this work.

https://doi.org/10.1016/j.virol.2018.10.013
Received 14 September 2018; Accepted 14 October 2018
Available online 26 October 2018
0042-6822/

latent infections usually characterised by an absence of clinical signs, thus representing a real risk to horse populations. As a consequence, economical losses linked to EHV infections are very significant, which warrants surveillance and prophylaxis (Kydd et al., 2012).

Several vaccines are available against EHV-1 and EHV-4. Although they reduce both clinical signs of the respiratory disease and virus shedding (Goodman et al., 2006), their efficacy against neurological disorders and abortion is limited (Kydd et al., 2012; Lunn et al., 2009; Patel and Heldens, 2005). Moreover, there is no vaccine against EHV-3. In view of these limitations, veterinary practitioners have turned toward alternative treatments and the use of antiviral is raising interest. Currently, no antiviral molecule has a marketing authorisation for equine species despite critical needs, warranting the development of new antiviral compounds or adaptation of drugs that are effective against human viruses (reviewed in Vissani et al., 2016). Two nucleoside analogues, aciclovir (ACV) and ganciclovir (GCV), are the most studied antiviral compounds against herpesviruses. *In vivo*, valaciclovir, which is the prodrug of ACV, was tested in experimental EHV-1 infection, but showed no antiviral effects (Garre et al., 2009). Quite surprisingly, the antiviral properties of GCV was never evaluated in horses despite interesting pharmacokinetic results (Carmichael et al., 2013). Nevertheless, both drugs were effective *in vitro* against EHV-1 (Garre et al., 2007), EHV-4 (Azab et al., 2010) and EHV-3 (Vissani et al., 2018), but the diversity of experimental designs and the lack of normalised assays make it difficult to compare the efficacy of these drugs on the different EHVs.

Conventional approaches for screening antivirals include the quantification of viral progeny in plaque assays, 50% tissue culture infective dose ($TCID_{50}$), or quantitative PCR, which are all time-consuming and tedious end-point assays. Alternative methods were developed to quantify cell protection from viral cytopathic effects by measuring either mitochondrial succinate-dehydrogenase activity with the MTT assay (Sudo et al., 1995), or intracellular ATP concentration with firefly luciferase (Noah et al., 2007). More recently, recombinant viruses expressing reporter proteins such as luciferase were also developed, but this approach is limited to viruses that can be modified by reverse genetics (Lucas-Hourani et al., 2014). In the last two decades, the use of label-free technologies in drug discovery received an increasing attention (Cooper, 2006). The Real-Time Cell Analysis (RTCA) system is an advanced label-free technology that measures cell growth using impedance variations in culture wells covered with gold electrodes (Solly et al., 2004). Impedance is modified by the presence of adherent cells in the wells, which can be used to monitor cell viability, migration, growth, spreading, proliferation and any modification due to viral cytopathic effect (Fang et al., 2011; Limame et al., 2012). A previous work investigated the applicability of RTCA to analyse the cytopathic effect of two different strains of EHV-1 infection (Golke et al., 2012). The current study is pushing further this approach by demonstrating that RTCA is a powerful technology for the evaluation of antivirals against EHV-1 but also EHV-4 and EHV-3, and is suitable for the screening of compound libraries when looking for new inhibitors of these viruses.

2. Materials and methods

2.1. Cells

Equine dermal (E. Derm; NBL-6) cells (ATCC® CCL57™, Manassas, VA) were maintained in Eagle's Minimum Essential Medium (EMEM; ATCC®) supplemented with 10% fetal bovine serum (Eurobio, Courtaboeuf, France), 100 IU/ml penicillin, 0.1 mg/ml streptomycin and 0.25 μg/ml amphotericin B (Eurobio) at 37 °C and 5% CO_2.

2.2. Viruses

Three EHV-1 strains were used throughout this study: Kentucky D (KyD) strain (ATCC® VR700™), isolate FR-6815 obtained from organs of an aborted fetus in 2013 (LABÉO, France), and isolate FR-38991 from the nasal swab of a horse with neurological disorders in 2009 (LABÉO, France). Two other EHVs strains were used: EHV-4 405/76 strain (ATCC® VR-2230™) and EHV-3 1118 strain (ATCC® VR-352™). The different multiplicities of infection (MOI) used in this study are indicated in Table 1.

Table 1
Multiplicity of infection used for each virus strains during equine dermal cells infection. M.O.I., Multiplicity of infection: the number of virus particles added per cell.

Virus (strain)	EHV-1 (KyD)[a]	EHV-1 (FR-6815)[b]	EHV-1 (FR-38991)[b]	EHV-4 (405/76)[a]	EHV-3 (1118)[a]
M.O.I. used	0.02	0.6	0.4	0.23	0.01

[a] : ATCC®.
[b] : LABÉO.

2.3. Chemical compounds

Aciclovir was purchased from Abcam (Cambridge, UK), ganciclovir, brequinar and spironolactone were purchased from Clinisciences (Nanterre, France). One plate from the Prestwick Chemical Library® (containing 80 compounds) was selected (part of the chemical libraries available on the CBC platform) as it contains aciclovir (well A07).

2.4. Cytotoxicity assay of chemical compounds

2.4.1. Trypan blue staining

Cell viability was measured at 48 h post-treatment (hpt) using a trypan blue solution at 0.4% (Ozyme, Montigny-le-Bretonneux, France), according to the manufacturer's instructions.

2.4.2. Luminescence-based viability assay

Cell viability was measured at 48 hpt using the CellTiter Glo® Luminescent Cell Viability Kit (Promega, Charbonnière-les-bains, France), according to the manufacturer's instructions. This assay quantifies ATP in culture wells, which reflects cellular metabolic activity. Signal was acquired using an Infinite® M200 luminometer (Tecan, Lyon, France).

2.5. Real-time cell monitoring of EHV-induced cytopathogenicity using RTCA

Real-time cell impedance was monitored using the RTCA MP system (ACEA Biosciences, Montigny le Bretonneux, France), with 6 independent positions for 96-well E-plates (ACEA Biosciences). The impedance signals measured by the electronic sensor analyser were derived in a dimensionless value, called Cell Index (CI) and graphically represented. The background readings were obtained with EMEM in each well of the E-plate view PET (ACEA Biosciences). Cells were then seeded at a density of 1.2×10^4 per well (adapted from Tian et al., 2012), incubated at room temperature for 30 min, and then placed onto the RTCA-MP station located in the incubator. CI values were measured automatically every minute during the first 10 h, and then every 15 min the next 14 h. After 24 h of incubation, medium was removed and cells were infected with the different EHV strains (Table 1) with or without chemical compounds. Negative controls were mock infected with medium and DMSO. Plates were put back onto the RTCA MP station, and the CI values were recorded every 10 min during 120 h. According to the manufacturer's recommendations, CI values were first normalised to match the last time point before cell infection using the RTCA software version 2.0 (ACEA Biosciences) prior to data analysis. Finally, three representative values were calculated for each culture conditions:

half maximal effective concentrations (EC_{50}), area under normalised curves (AUC_n; Pan et al., 2013), and times required for the CI to decrease by 50% after virus infection ($CIT_{50;}$ Fang et al., 2011). The quality of the screening in 96-well format was warranted using the Z′-factor calculation (Zhang et al., 1999) based on AUC_n values between 0 and 120 h post-infection (hpi). The formula is: $Z' = 1–3 \times (\sigma^+ + \sigma^-) \div (\mu^+ - \mu^-)$, where σ^+ and σ^- correspond to standard deviations of AUC_n for uninfected and infected cells with DMSO, respectively; and μ^+ and μ^- correspond to means of AUC_n for uninfected and infected cells with DMSO, respectively. Z′-factor is expected to be above 0.5, or the corresponding plate is discarded.

2.6. Nucleic acids and qPCR

In parallel to each real-time monitoring, 96 well plates were prepared with the same culture conditions as outlined above to perform qPCR. Cell cultures were frozen at −20 °C at different time points: 0, 24 and/or 48 hpi. Nucleic acids were extracted with the QIAamp® Viral RNA Mini Kit (Qiagen, Courtaboeuf, France) according to the manufacturer's instructions and stored at −20 °C until used. Quantitative PCR protocols for EHV-1, EHV-4 and EHV-3 adapted from the standard NF U47-600-2 have been previously described (Hue et al., 2016). Each reaction was processed in a total volume of 25 µl containing 2× Taqman® Universal PCR Master Mix (Life Technologies, Villebon-sur-Yvette, France), primers and probes (Table 2). Each thermal cycling described in Table 2 was performed on a QuantStudio™ 12 K Flex Real-Time PCR System (Life Technologies).

2.7. Cell morphology analysis

For both assays, cell morphology and viral cytopathic effects (CPE) were observed using the inverted Eclipse Ti microscope (Nikon, Champigny sur Marne, France). Apoptosis tests were observed using IncuCyte S3 (Essen Bioscience, Ann Arbor, Michigan, USA) with IncuCyte Caspase 3/7 Green Reagent (Essen Bioscience).

2.8. Statistical analyses

Statistical analyses were performed with the GraphPad Prism® software version 6.0 (La Jolla, CA, USA). Data are expressed as mean ± standard deviation (SD). Normality of continuous data distribution was evaluated using the Kolmogorov–Smirnov test. Viral loads being not normally distributed were log-transformed before comparison by ANOVA, with Tukey and Dunnett post hoc tests when appropriate. Cell viability tests were compared using ANOVA, with Bonferroni and Dunn post hoc tests when appropriate. Values of $P < 0.05$ were considered statistically significant.

3. Results

3.1. Real-time monitoring of EHV-1-induced cytopathic effects

Cytopathic effect induced by EHV-1 (KyD strain) infection of E. Derm cells was monitored by RTCA (Fig. 1A). From 24 h before infection (seeding step) to 20 h before infection, the normalised cell index (CI_n) rapidly increased due to cell adhesion. From 20 h before infection to the infection time (0 h), CI_n values slowly increased as a result of cellular proliferation, and this continued over time for mock-infected cells (Fig. 1A; red curve). In infected culture conditions, the CI_n began to decrease from 24 hpi (Fig. 1A; purple curve), which corresponds to the first virus-mediated cytopathic effects (CPE) visualised by microscopic observation (Fig. 1C - 24 hpi). The decrease in the CI_n values intensified to reach zero at 48 hpi (Fig. 1A), with no more adherent cells present in the culture (Fig. 1C - 48 hpi). In parallel, viral growth was measured by qPCR at 0, 24 and 48 hpi (Fig. 1B). EHV-1 genome copies increased significantly ($P < 0.001$) and gradually in line with virus-mediated CPE formation and inversely with the CI_n decreasing. However, no alteration in cell viability was observed at 48 hpi in infected conditions, when measured by trypan blue staining or ATP quantification (Supplementary Fig. 1A and B, respectively). Moreover, no cleavage of Caspases 3/7 was observed during the first 48 h of infection (Supplementary Fig. 1C).

3.2. Effect of aciclovir and ganciclovir against three different EHV-1 strains

The absence of cytotoxicity was confirmed for ACV and GCV at the different concentrations tested (Supplementary Fig. 2). Antiviral effect of ACV or GCV against the EHV-1 KyD strain was evaluated by RTCA. Results showed that ACV prevented the CI_n decrease induced by EHV-1 infection in a dose-dependent manner (Fig. 2A). Aciclovir significantly reduced the number of viral genome copies in EHV-1 infected E. Derm cells by 1.5 $\log_{10}$ ($P < 0.001$) and 2.8 $\log_{10}$ ($P < 0.001$) at 5 µg/ml and 50 µg/ml, respectively (Fig. 2B). Ganciclovir was even more potent as concentrations of 0.5–50 µg/ml strongly limited the CI_n decrease induced by EHV-1 infection (Fig. 2C), whereas a concentration of 0.05 µg/ml slightly delayed the CI_n decrease induced by EHV-1 infection. Quite similarly, GCV significantly reduced the number of viral genome copies by 1.5 $\log_{10}$ ($P < 0.001$), 2.4 $\log_{10}$ ($P < 0.001$) and 2.4 $\log_{10}$ ($P < 0.001$) at 0.5 µg/ml, 5 µg/ml and 50 µg/ml, respectively (Fig. 2D). The cell morphology profiles observed by microscopy support these results (Fig. 2E). The susceptibility of two other EHV-1 strains (FR-6815 and FR-38991) to ACV and GCV was evaluated in E. Derm cells by RTCA and qPCR, and corroborate the results obtained the KyD strain (Fig. 2F). No significant difference ($P < 0.001$) was observed between the three different EHV-1 isolates (Fig. 2F; mean EC_{50} ± SD at 48 hpi). Furthermore, and regardless of the method used, the EC_{50} values for GCV (RTCA mean value: 1.01 ± 0.53 µg/ml) were approximatively 10-fold lower than for ACV (RTCA mean value: 10.28 ± 2.31 µg/ml).

Table 2
Sequences of primers, probes and amplification programs used for the detection of equid alphaherpesviruses. F: forward primer; R: reverse primer; P: probe; MGB: minor groove binder.

Targets	Primers and probes sequences (5′-3′)	Amplification programs		References
EHV-1	F: CATGTCAACGCACTCCCA	95 °C 10 min		Adapted from (Diallo et al., 2006)
	R: GGGTCGGGCGTTTCTGT	95 °C 15 s	x 40	
	P: FAM-CCCTACGCTGCTCC-MGB	62 °C 1 min		
EHV-4	F: GGGCTATTGGATTACAGCGAGAT	95 °C 10 min		Adapted from (Diallo et al., 2007)
	R: TAGAATCGGAGGGCGTGAAG	95 °C 15 s	x 40	
	P: FAM-CAGCGCCGTAACCAG-MGB	60 °C 1 min		
EHV-3	F: GACGGTCACCACGATCG	95 °C 10 min		Adapted from (Léon et al., 2008)
	R: GGCCAACTTTCCCGAG	95 °C 15 s	x 40	
	P: FAM-GCGAGACATGCTGCTAGGCA-MGB	60 °C 1 min		

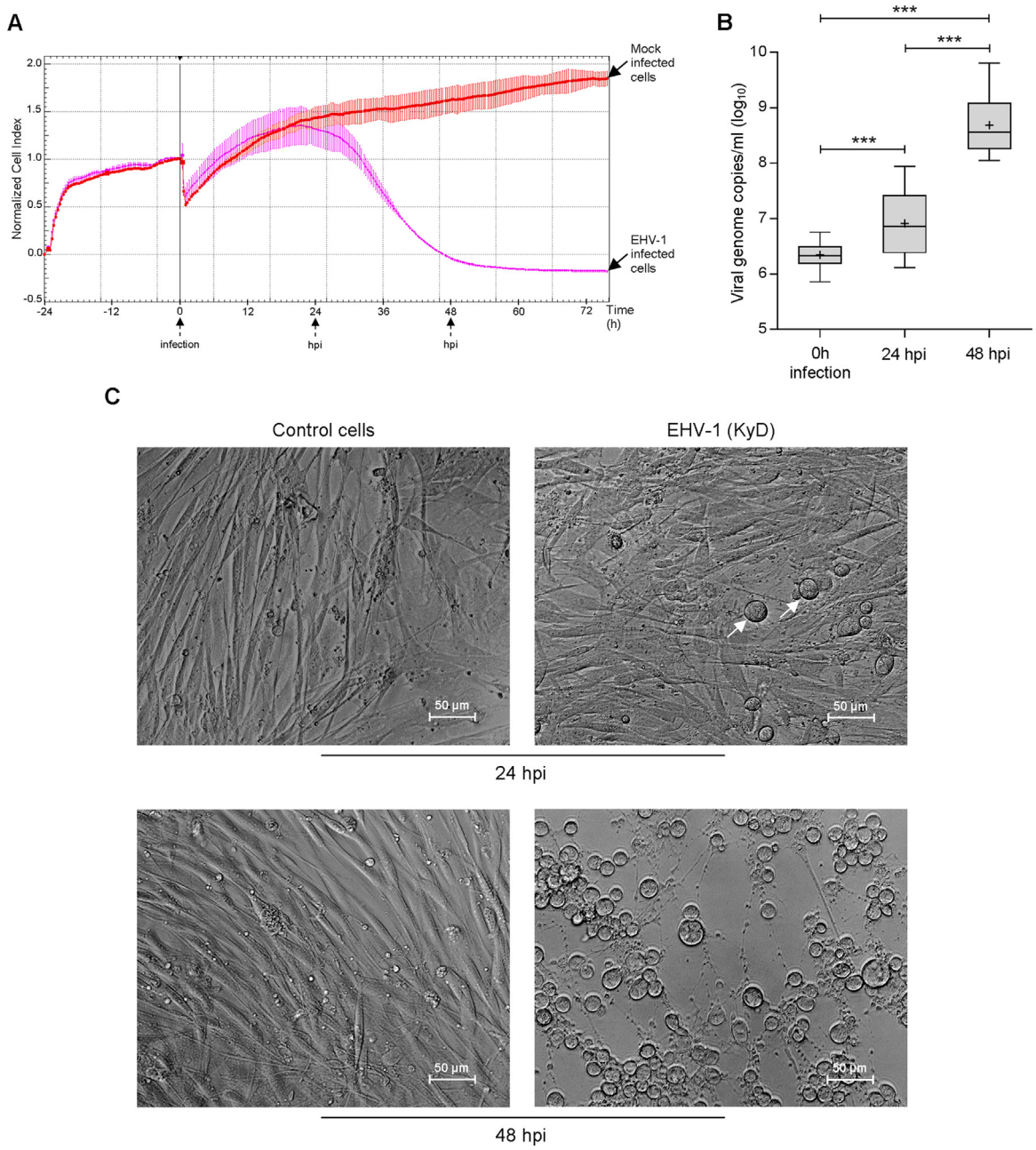

Fig. 1. Effect of EHV-1 KyD strain on E. Derm cells. (**A**) Real time monitoring of E. Derm cells proliferation and effect of CPE induced by EHV-1 measured by RTCA. The Cell Index values are normalised at the last time point before infection of cells (black vertical line). The red curve represents the CI_n of mock infected cells and purple curve represents the CI_n of EHV-1 infected cells. Each data point indicates the mean ± SD of one assay in duplicate. Three independent experiments were performed. (**B**) Viral genome copies of EHV-1 measured by qPCR assays in the supernatant of infected cells collected at 0, 24 and 48 hpi. Box-plots represent the $\log_{10}$ of viral genome copy numbers of twenty-two independent experiments (***: $P < 0.001$). (**C**) Microscopic observation of E. Derm cells infected or not by EHV-1 at 24 hpi and 48 hpi. White arrow indicates CPE.

3.3. Effect of aciclovir and ganciclovir against EHV-4 and EHV-3

The antiviral activity of ACV and GCV was tested on two other alphaherpesviruses: EHV-4 (strain 405/76) and EHV-3 (strain 1118). E. Derm cells were infected with EHV-4 (Fig. 3) or EHV-3 (Fig. 4) in the absence or presence of ACV or GCV, and the CI_n values were determined from 0 to 72 hpi. The CI_n values decreased upon EHV-4 infection, and both ACV and GCV showed cell protective effects (Fig. 3A and B). Antiviral effects were confirmed by quantification of viral genome copies at 48 hpi (Fig. 3C and D), in line with cell morphology profiles observed by microscopy (Fig. 3E). For EHV-4 infection, the EC_{50} values determined by RTCA were 17.38 ± 5.95 µg/ml for ACV and 2.79 ± 0.25 µg/ml for GCV. When determined by qPCR, the EC_{50} values for ACV and GCV against EHV-4 were 2.83 ± 1.80 µg/ml and 0.36 ± 0.16 µg/ml, respectively. Similar results were obtained with EHV-3 (Fig. 4A-E). The EC_{50} values determined by RTCA for ACV and GCV (calculated by RTCA) were 15.23 ± 2.85 µg/ml and 1.86 ± 0.46 µg/ml, respectively (Fig. 4A-B). When calculated by qPCR, the EC_{50} values for ACV and GCV against EHV-3 were 1.92 ± 1.90 µg/ml and 0.55 ± 0.20 µg/ml, respectively (Fig. 4C-D). Again, results were supported by cell morphology profiles observed by microscopy (Fig. 4E).

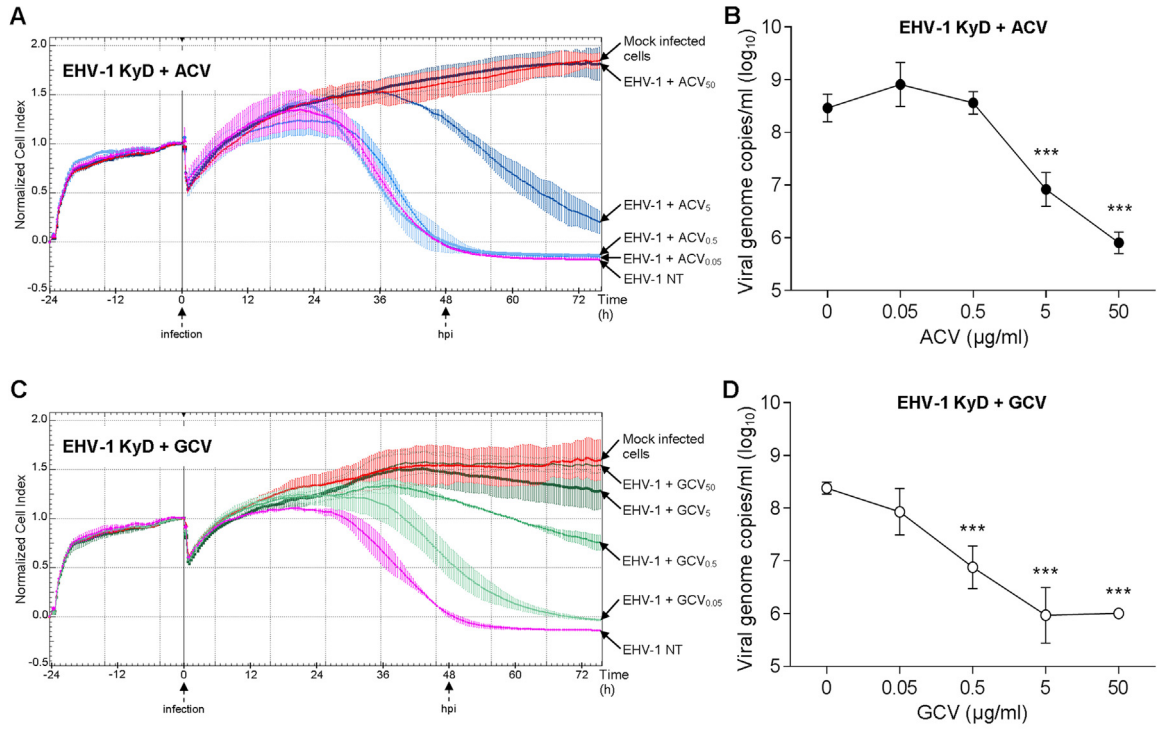

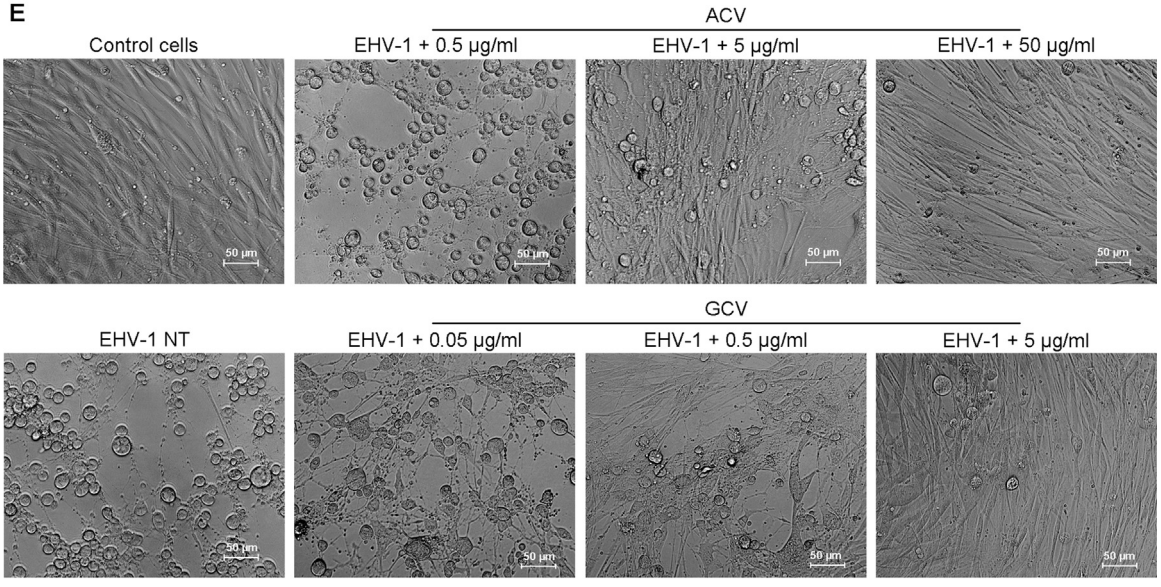

F

	EC_{50} ± SD (µg/ml)			
	ACV		GCV	
EHV-1 strain	RTCA	qPCR	RTCA	qPCR
KyD	9.88 ± 2.14	2.50 ± 0.92	0.62 ± 0.49	0.07 ± 0.04
6815	10.67 ± 2.15	2.13 ± 1.21	1.32 ± 0.44	0.29 ± 0.05
38991	10.30 ± 3.15	2.27 ± 1.77	1.11 ± 0.52	0.29 ± 0.40
Mean values ± SD	10.28 ± 2.31	2.30 ± 1.22	1.01 ± 0.53	0.21 ± 0.24

(caption on next page)

Fig. 2. Effects of ACV and GCV on E. Derm cells infected by EHV-1 (KyD). Real time monitoring of E. Derm cells infected by EHV-1 and treated by ACV (**A**) and GCV (**C**) measured by RTCA. The Cell Index values are normalised at the last time point before infection of cells (black vertical line). The red curve represents the CI_n of mock infected cells and purple curve represents the CI_n of EHV-1 infected cells and untreated (NT). Blue and green shade curves represent the CI_n of EHV-1 infected cells and treated with ten-fold serial dilution of ACV and GCV (50–0.05 μg/ml), respectively. Each data point indicates the mean ± SD of one assay in duplicate. Three independent experiments were performed. Viral genome copies of EHV-1 in the culture supernatant 48 hpi measured by qPCR assays after ACV (**B**) and GCV (**D**) treatments. Each point represents the mean ± SD of the $\log_{10}$ of viral genome copy numbers of three independent experiments (***: $P < 0.001$). NT: not treated. (**E**) Microscopic observation at 48 hpi of E. Derm cells infected or not by EHV-1 after ACV or GCV treatment. (**F**) Susceptibility of three different EHV-1 strains to antiviral compounds measured by RTCA and qPCR at 48 hpi. Results are the means ± SD of four independent experiments. Mean values correspond to mean of twelve EC_{50} values. EC_{50}: 50% effective concentration; qPCR: quantitative PCR.

3.4. Real-time cell analysis screening of antiviral compounds against EHV-1

In order to evaluate the RTCA system for the high-throughput screening of antiviral molecules in a 96-well format, a set of 80 chemical compounds was prepared at the Institut Pasteur, and then tested in our laboratory against EHV-1 infection (KyD strain) under blind conditions. All compounds were screened at 10 μg/ml because this concentration fits the EC_{50} of ACV as determined above (Fig. 2F). Ganciclovir (wells E12 - F12) was used as a positive antiviral control, whereas brequinar (wells G12 - H12), which kills E. Derm cells at 50 μg/ml, was used as a cytotoxicity control. Data were analysed according to the decision tree presented in Fig. 5A. For each well, the area under the normalised curve (AUC_n) is calculated in order to integrate all CI_n values acquired by RTCA from 0 to 120 hpi (Fig. 5B). AUC_n values were ranging from 174.12 ± 12.20 for non-infected cells to 54.95 ± 4.24 for EHV-1 infected cells, with GCV showing some protective effect as expected (AUC_n = 150.68 ± 4.23) while brequinar showing cytotoxic effect (AUC_n = 13.89 ± 0.58). The Z′-Factor calculated from AUC_n values was found to be 0.59. Analysis of the RTCA curves indicated that compared to infected control cells, CI_n values prematurely declined with nine compounds and were not considered as potential antiviral compounds against EHV-1. Based on the AUC_n results, coupled with the time required for the CI to decrease by 50% after virus infection (CIT_{50}), only two compounds (aciclovir (A07) and spironolactone (E09)) scored positive among the 71 remaining compounds and delayed the CIT_{50} by 36 h 06 min and 07 h 51 min, respectively. Viral growth and microscope observations were performed at 48 hpi and showed that spironolactone decreased by 1.4 $\log_{10}$ the EHV-1 genome copies number at 10 μg/ml (Fig. 5C) and delayed EHV-1 induced CPE on E. Derm cells (Fig. 5D). The antiviral effect of spironolactone was confirmed by three independent experiments with two-fold serial dilutions (Fig. 6). The EC_{50} values for spironolactone against EHV-1 were 11.24 ± 0.51 μg/ml determined by RTCA and 4.06 ± 1.58 μg/ml calculated by qPCR. Results were supported by cell morphology profiles observed by microscopy (Fig. 6).

4. Discussion

The main methods for identifying antivirals are end-point assays, such as cell viability measurement, using colorimetric assays and microscopic monitoring. These methods are usually time-consuming and may not be adapted to study the cytopathic effect induced by EHV-1 on E. Derm cells. In our study, EHV-1 did not induce a loss of viability at 48 hpi when measured by trypan blue staining assays or ATP quantification (Supplementary Fig. 1). In fact, infected cells change their morphology by rounding up, and while adhesion to the substrate is lost, cells remain metabolically active to replicate the virus. The absence of cleavage of Caspases 3/7 during the first 48 hpi is consistent with previous studies. Turowska et al. (2010) reported that EHV-1 infection induces alterations in the cytoskeleton but does not trigger apoptosis in E. Derm cells at 24 hpi. More recently, Scrochi et al. (2017) showed that EHV-1 down-regulates apoptosis in E. Derm cells, but the mechanism involved is not yet defined. As conventional methods are not adapted in our conditions, a new approach has been investigated. Monitoring of cells impedance using electric field was first established in the 1980s (Giaever and Keese, 1993, 1984). Since then, the use of this technology in the field of virology clearly increased, as impedance measurement appears to be an effective tool to study CPE (Charretier et al., 2018; Fang et al., 2011; Marlina et al., 2015; Pennington and Van de Walle, 2017; Piret et al., 2016; Spiegel, 1993; Teng et al., 2013; Tian et al., 2012; Witkowski et al., 2010). In this study, RTCA was used for the first time to follow the formation of CPE induced by three equid alphaherpesvirus species on E. Derm cell cultures, to measure the activity of two conventional antiviral compounds against these three viruses, and finally to conduct a pilot screen of eighty chemical compounds against EHV-1.

Results reported here further support the use of RTCA to monitor in real-time the CPE formation induced by EHV-1 on E. Derm cells, in line with the previous report of Golke et al. (2012), but also extend the application of this technology to EHV-4 and EHV-3. Furthermore, we showed that antiviral effects of reference drugs could be precisely quantified using the RTCA technology. First of all, CI_n decrease was positively correlated with CPE formation, as characterised by morphological changes and detachment of the cells. Secondly, viral loads measured by qPCR were negatively correlated with CI_n values as assessed in EHV-1, EHV3 or EHV-4 infected cultures when treated with ACV or GCV. These results are also consistent with previous observations on herpes simplex virus 1 (Piret et al., 2016), and confirm the interest of RTCA for monitoring the infection of permissive cells with herpesviruses. A recent study has also used impedance as a read-out to monitor cellular infections by the felid herpesvirus type 1, but using the Electric Cell-substrate Impedance Sensing system (ECIS, Applied BioPhysics; Pennington and Van de Walle, 2017). Although the ECIS and RTCA measurement systems present some differences, the impedance profiles obtained for uninfected and infected cells using the two systems are concordant. With the ECIS system, the users must determine the appropriate frequency to evaluate resistance, capacitance and impedance levels, while with the RTCA system, the impedance level is automatically determined.

Aciclovir and ganciclovir are first-line antiviral compounds for the treatment of herpes simplex viruses and human cytomegalovirus diseases, respectively (De Clercq, 2013; De Clercq and Li, 2016), and are both active against EHV-1, EHV-4 and EHV-3 *in vitro* (reviewed in Vissani et al., 2016). In this study, the multiplicity of infection was set for each EHV-1 strain in order to have 100% of infected cells at 48 hpi. MOIs of the two field isolates (FR-6815 and FR-38991) were similar, whereas the MOI of the KyD strain was approximately 25 times lower. The referent KyD strain was isolated more than five decades ago, and compared to field strains, seems very well adapted to cell culture, which probably explains that a lower MOI had to be used. According to EC_{50} data calculated for ACV and GCV, no difference in sensitivity was measured between the three EHV-1 strains studied here. Strain FR-38991 was isolated in a previous study during an EHM episode (Pronost et al., 2012) and possess the A_{2254} mutation in the ORF30 DNA polymerase gene, as the KyD reference strain, whereas strain FR-6815 more recently isolated from an abortion episode does not. This observation is consistent with a previous report using a plaque reduction assay (PRA) with six EHV-1 isolates (Garre et al., 2007). The EC_{50} measured by qPCR are similar to EC_{50} measured by PRA for both ACV and GCV on equine embryonic lung cells (Garre et al., 2007) and primary fetal horse kidney (Azab et al., 2010). In contrast, EC_{50} calculated by RTCA were approximately 10 times higher than EC_{50} calculated by qPCR. The main

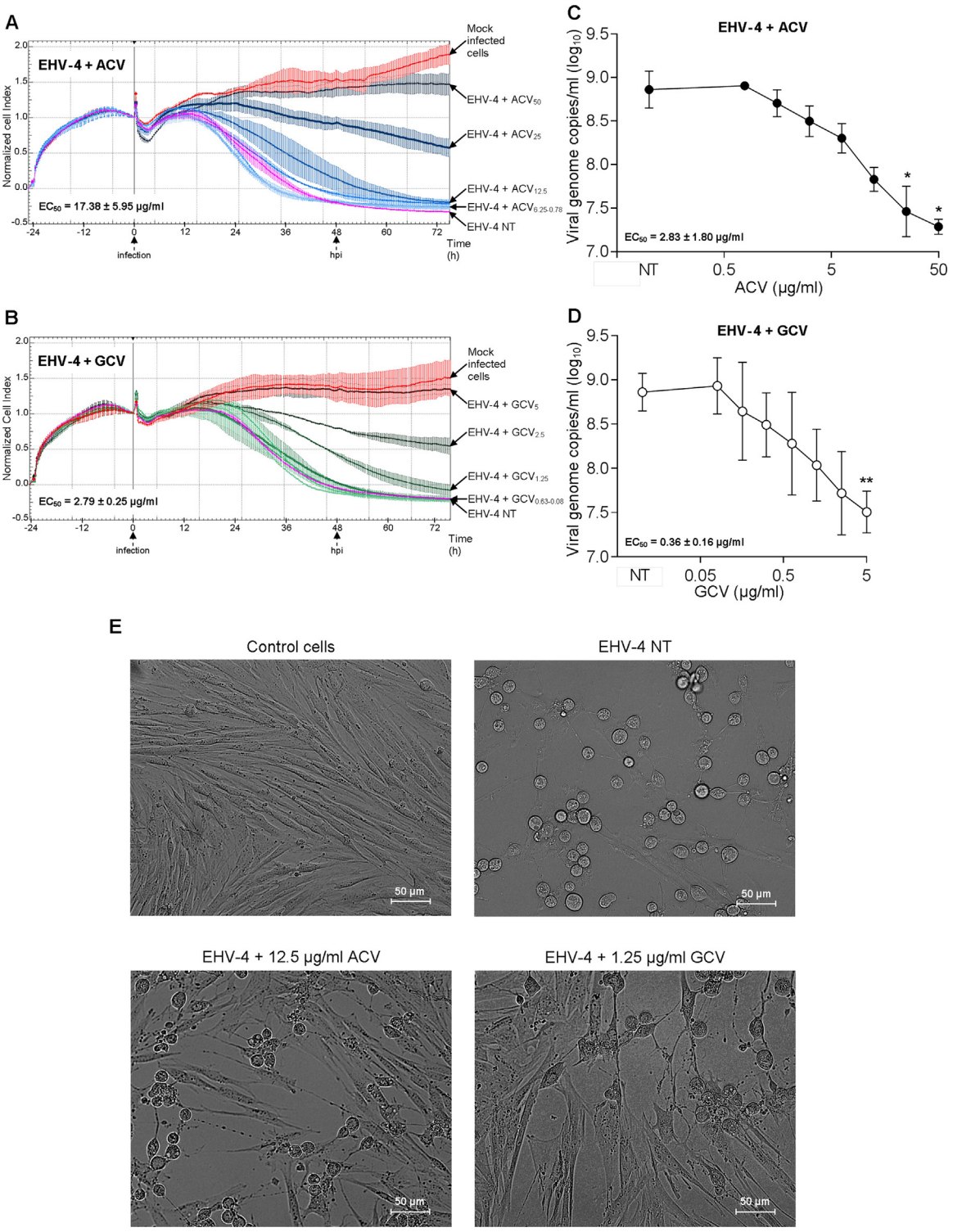

Fig. 3. Susceptibility of EHV-4 to ACV and GCV treatments measured by RTCA and qPCR. Real time monitoring of the susceptibilities of EHV-4 405/76 strain to ACV (**A**) and GCV (**B**) treatments on E. Derm cells. The Cell Index values are normalised at the last time point before infection of cells (black vertical line). The red curve represents the CI_n of mock infected cells and purple curve represent the CI_n of cells infected with EHV-4. Blue shade curves represent the CI_n of cells treated with two-fold serial dilution of ACV (50–0.78 µg/ml) and green shade curves represent the CI_n of cells treated with two-fold serial dilution of GCV (5–0.08 µg/ml) after infection by EHV-4. Each data point indicates the mean ± SD of one assay in duplicate. Three independent experiments were performed. The EC_{50} were determined at 48 hpi for three independent experiments. Viral genome copies number of EHV-4 measured by qPCR at 48 hpi after treatment with different concentrations of ACV (**C**) and GCV (**D**). Each point represents the mean ± SD of the $\log_{10}$ viral copy numbers of three independent experiments (*: $P < 0.05$, **: $P < 0.01$). (**E**) Microscopic observation at 48 hpi of E. Derm cells infected or not by EHV-4 after ACV (12.5 µg/ml) and GCV (1.25 µg/ml) treatment. NT: not treated.

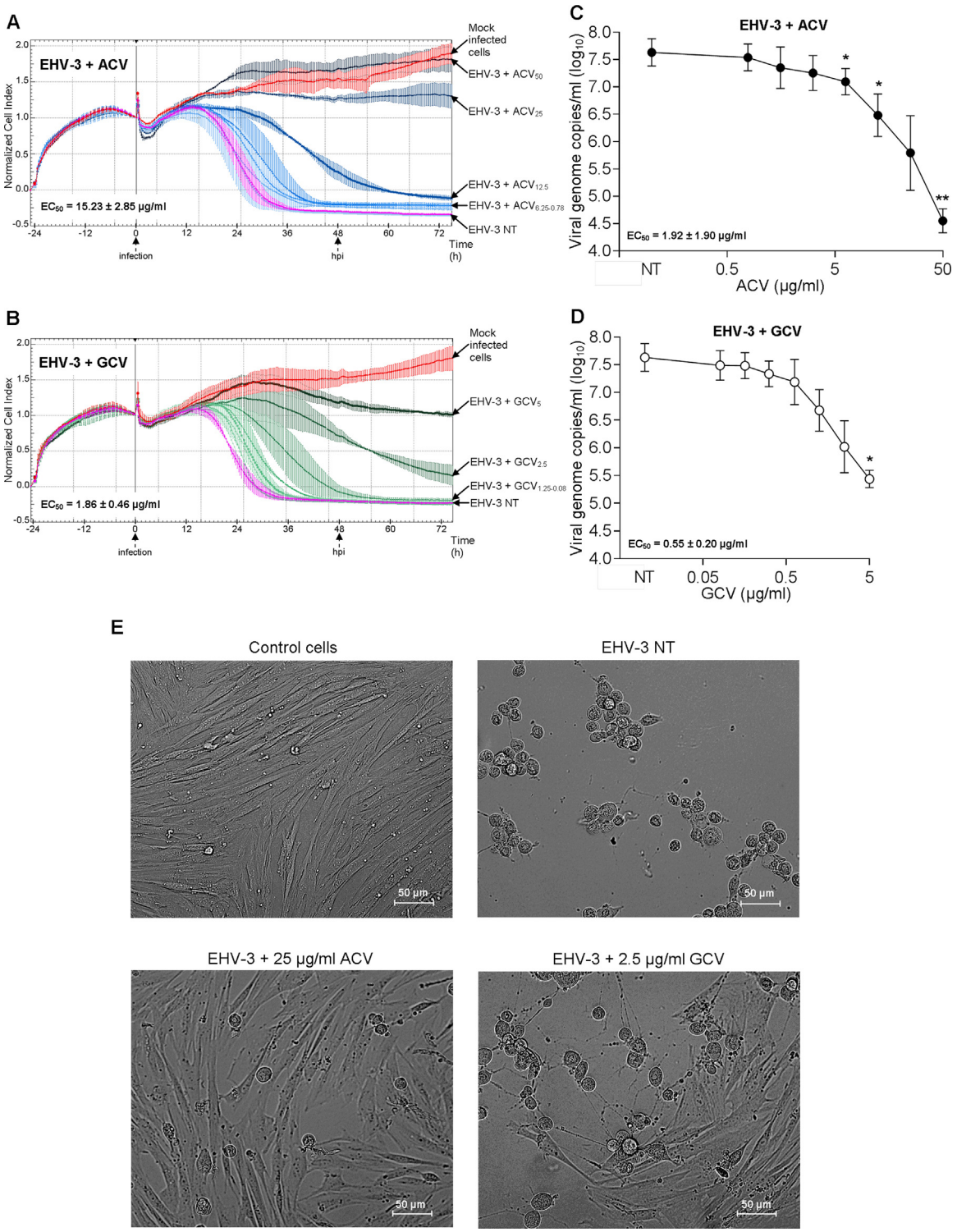

Fig. 4. Susceptibility of EHV-3 to ACV and GCV treatments measured by RTCA and qPCR. Real time monitoring of the susceptibilities of EHV-3 1118 strain to ACV (**A**) and GCV (**B**) treatments on E. Derm cells. The Cell Index values are normalised at the last time point before infection of cells (black vertical line). The red curve represents the CI_n of mock infected cells and purple curve represent the CI_n of cells infected with EHV-3. Blue shade curves represent the CI_n of cells treated with two-fold serial dilution of ACV (50–0.78 µg/ml) and green shade curves represent the CI_n of cells treated with two-fold serial dilution of GCV (5–0.08 µg/ml) after infection by EHV-3. Each data point indicates the mean ± SD of one assay in duplicate. Three independent experiments were performed. The EC_{50} were determined at 48 hpi for three independent experiments. Viral genome copies number of EHV-3 measured by qPCR at 48 hpi after treatment with different concentrations of ACV (**C**) and GCV (**D**). Each point represents the mean ± SD of the $\log_{10}$ viral copy numbers of three independent experiments (*: $P < 0.05$, **: $P < 0.01$). (**E**) Microscopic observation at 48 hpi of E. Derm cells infected or not by EHV-4 after ACV (25 µg/ml) and GCV (2.5 µg/ml) treatment. NT: not treated.

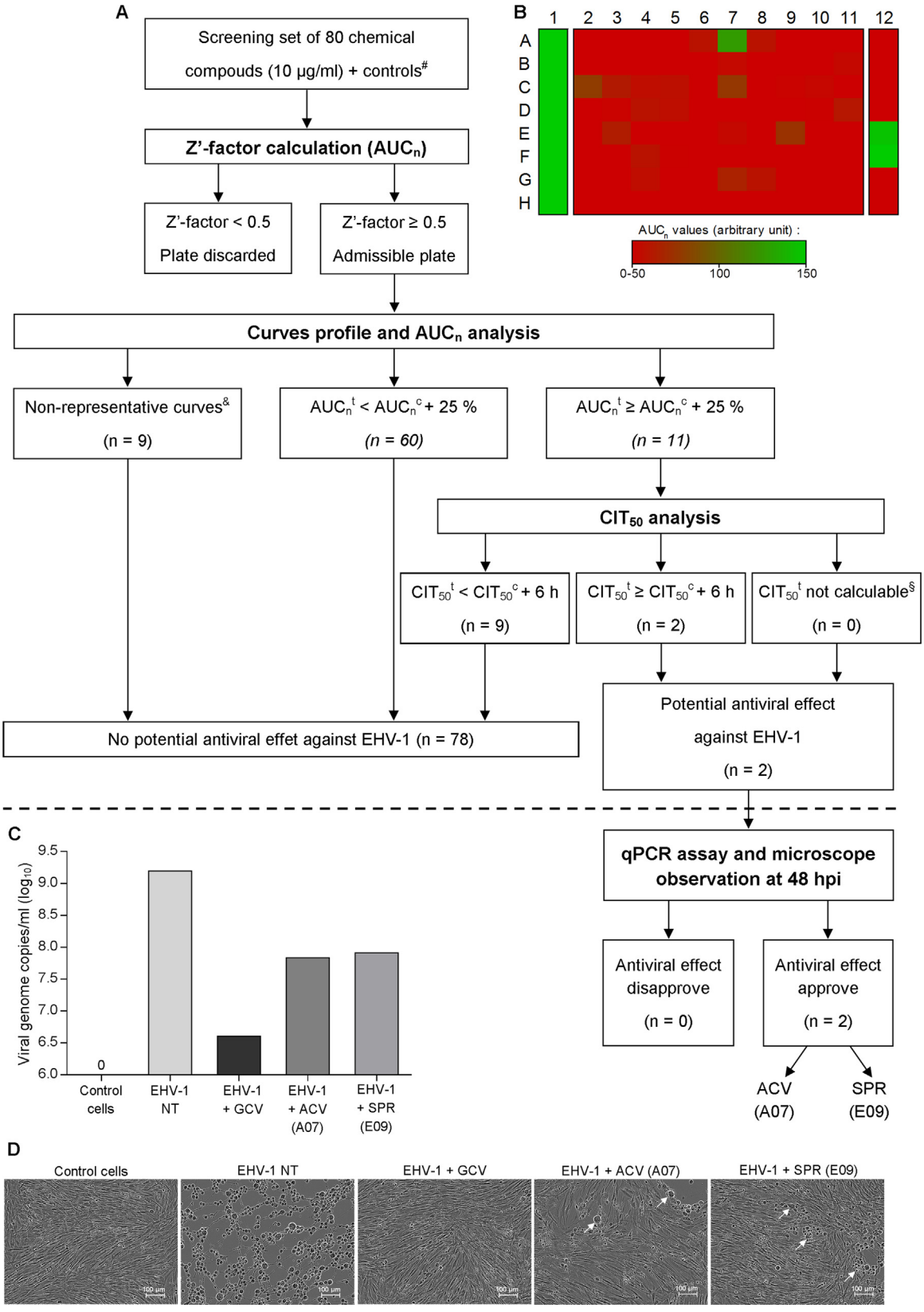

(caption on next page)

reason to explain the variation in EC_{50} could be related to the different readouts of these techniques (*i.e.* cellular adherence level measured by RTCA *versus* genome copies numbers measured by qPCR). Although the anti-EHV-1 effects of ACV and GCV were clearly demonstrated, results show that GCV was the most effective against all three EHV-1 strains compared to ACV. Indeed, GCV was between 10 and 20-times more effective than ACV against EHV-1. Our results confirm previous studies where GCV was found to be 12 times (Garre et al., 2007) and 27 times

Fig. 5. Analysis of one chemical library screening in 96-well format. (**A**) Decision tree for data analysis from chemical library screening in 96-well format using RTCA. 80 compounds were tested (columns 2–11). Columns 1 and 12 are devoted to controls, which are used to determine the Z′-factor calculated from the area under normalised curves (AUC_n) values between 0 hpi and 120 hpi. AUC_n^t is the area under normalised curves of treated cells, AUC_n^c is the area under normalised curves of untreated controls cells, CIT_{50}^t is the time required to the CI_n of treated cells to decrease 50% after virus infection and CIT_{50}^c is the time required to the CI_n of untreated controls cells to decrease 50% after virus infection. # Controls correspond to infected/uninfected cells with or without DMSO, infected cells with 5 µg/ml GCV and uninfected cells with 50 µg/ml brequinar. & Non-representative curves: curves with a decline of CI_n values that appear prior CPE formation (example: brequinar at 50 µg/ml). § CIT_{50}^t not calculable: treatments prevent the CI_n decrease (example: ganciclovir at 5 µg/ml). Dashed line separates the screening step from the validation step. (**B**) Heat map representation of the plate from the Prestwick Chemical Library® (80 compounds) screened at 10 µg/ml under blind conditions. AUC_n corresponds to the area under curves calculations after CI normalisation between 0 hpi and 120 hpi. Column 1 corresponds to uninfected control cells either untreated (wells A1 - D1) or treated with DMSO (wells E1 - H1), and column 12 corresponds to infected cells (wells A12 - B12), infected cells with DMSO (wells C12 - D12), infected cells with 5 µg/ml GCV as positive antiviral control (wells E12 - F12) and uninfected cells with 50 µg/ml brequinar as a toxicity control (wells G12 - H12). (**C**) Viral genome copies number of EHV-1 measured by qPCR at 48 hpi after treatment with 5 µg/ml of GCV, 10 µg/ml of ACV and 10 µg/ml of spironolactone (SPR). Each bar represents the $\log_{10}$ viral copy numbers of a single experiment. (**D**) Microscopic observation at 48 hpi of E. Derm cells infected or not by EHV-1 after GCV (5 µg/ml), ACV (10 µg/ml) and SPR (10 µg/ml) treatments. White arrow indicates CPE induced by EHV-1. NT: not treated.

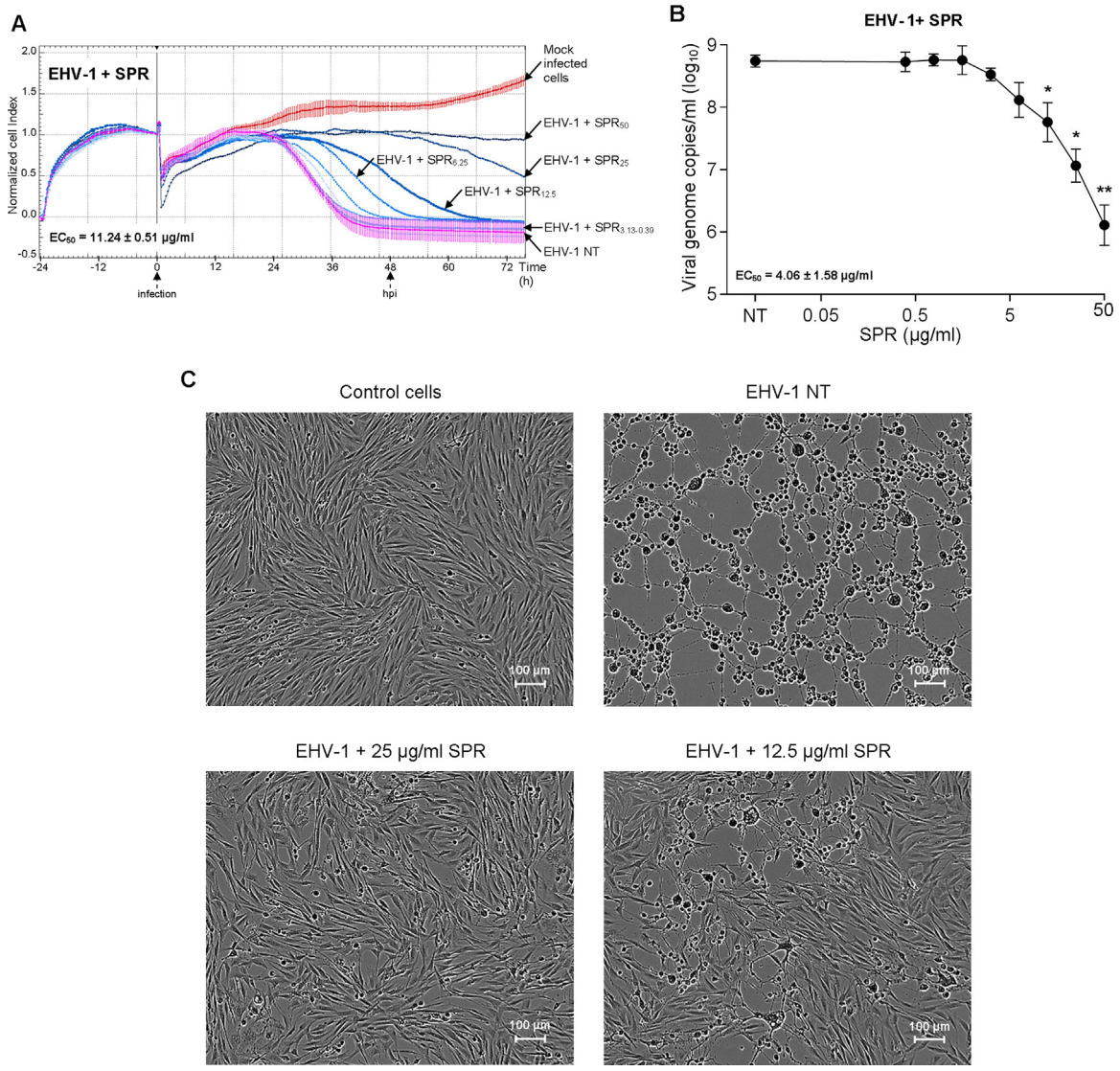

Fig. 6. Susceptibility of EHV-1 to spironolactone treatment measured by RTCA and qPCR. (**A**) Real time monitoring of the susceptibility of EHV-1 KyD strain to spironolactone (SPR) treatment on E. Derm cells. The Cell Index values are normalised at the last time point before infection of cells (black vertical line). The red curve represents the CI_n of mock infected cells and purple curve represent the CI_n of cells infected with EHV-1. Blue shade curves represent the CI_n of cells treated with two-fold serial dilution of SPR (50–0.39 µg/ml) after infection by EHV-1. The EC_{50} were determined at 48 hpi for three independent experiments. (**B**) Viral genome copies number of EHV-1 measured by qPCR at 48 hpi after treatment with different concentrations of SPR. Each point represents the mean ± SD of the $\log_{10}$ viral copy numbers of three independent experiments (*: $P < 0.05$, **: $P < 0.01$). (**C**) Microscopic observation at 48 hpi of E. Derm cells infected or not by EHV-1 after SPR (25 µg/ml and 12.5 µg/ml) treatment. NT: not treated.

(Azab et al., 2010) more effective than ACV in PRA, which supports the use of RTCA for antiviral studies.

Although several studies have evaluated the effectiveness of ACV and GCV against EHV-1 *in vitro*, there are only few available data concerning their activities against EHV-4 or EHV-3. Using RTCA, we have demonstrated that EHV-4 is sensitive to ACV and GCV. Although, EHV-4 is closely related to EHV-1, it appears slightly less sensitive to these antiviral compounds. Our data are consistent with the previous report by (Azab et al., 2010) showing an EC_{50} value higher than 50 μg/ml for the TH20p strain after ACV treatment. Concerning EHV-3, the EC_{50} of ACV treatment obtained by RTCA is consistent with the one obtained by PRA in the same cellular model (15.74 ± 4.48 μg/ml; Vissani et al., 2018). Our results also confirm that EHV-3 is more sensitive to GCV than ACV, although the EC_{50} of GCV obtained by RTCA was 10 times higher compared to PRA (Vissani et al., 2018). Based on these results, GCV is the best antiviral compound against these three alphaherpesviruses *in vitro* and appears promising for *in vivo* experiments.

As it is allowing the independent monitoring of 6 × 96-well plates, the RTCA MP instrument is adapted to conduct functional screenings for antiviral compound discovery, saving significant time and energy, when compared with other methods. RTCA automatically accumulates strong kinetic data requiring the calculation of appropriate parameters. In this study, a pilot screen of eighty compounds on one 96-well plate was conducted against EHV-1. Fig. 5 presents our decisional tree to interpreting the screening data using RTCA system. The Z′-factor is a useful tool to determine the quality of high-throughput screening (Zhang et al., 1999). Based on AUC_n results, the Z′-Factor value was found above 0.5, which proves the high robustness of this assay. The AUC_n calculation coupled to curves analysis and CIT_{50} determination allow highly sensitive analyses of RTCA screening results. Indeed, our system was effective to pinpoint ACV among eighty compounds under blind conditions and discovered spironolactone as a new potential inhibitor of EHV-1. The effect of spironolactone was confirmed by dose-response assays against EHV-1, but also EHV-4 and EHV-3 (data not shown). These results suggest that this molecule could inhibit different *Herpesviridae*. Interestingly, Verma et al. (2016) had recently reported that spironolactone reduced the production of Epstein-Barr virus, a major human *Herpesviridae,* by targeting the SM protein. The antiviral effect of spironolactone was also reported in RNA viruses (HIV-1 and HIV-2; (Lacombe et al., 2016). Spironolactone is a mineralocorticoid antagonist and potassium-sparing diuretic, used in the treatment of high blood pressure, heart failure and dropsy (Chapman et al., 2007; Pitt and Perez, 1999). It is also an androgen signalling inhibitor frequently used in the treatment of various dermatological conditions that involve testosterone (Trivedi et al., 2017). This demonstrates the interest of RTCA for the phenotypic screening of chemical libraries to identify antivirals.

In summary, this study confirms the efficiency of RTCA to monitor CPE formation induced by EHV-1 on E. Derm cells, and further extends this tool to EHV-4 and EHV-3. It is also the first evaluation and comparison of antiviral compounds against equid alpha-herpesviruses using a unique cell line and a normalised assay. In this model, GCV was found more effective than ACV against all viruses used to infect E. Derm cells. Furthermore, this label-free technology was proven suitable for the high-throughput screening of antiviral compounds, and allowed the identification of spironolactone as a novel inhibitor of EHV-1. In conclusion, RTCA technology is a promising and powerful tool allowing to complement and support conventional methods used in the field of equine virology.

Acknowledgments

This work was supported by LABÉO, IFCE (Institut Français du Cheval et de l'Equitation, project AMIE), Fonds Eperon (project N87-2014, N07-2015, N07-2016 and N13-2017) and Région Normandie (CPER R25 P3).

Conflict of interest

The authors declare no competing interests.

Appendix A. Supporting information

Supplementary data associated with this article can be found in the online version at doi:10.1016/j.virol.2018.10.013

References

Azab, W., Tsujimura, K., Kato, K., Arii, J., Morimoto, T., Kawaguchi, Y., Tohya, Y., Matsumura, T., Akashi, H., 2010. Characterization of a thymidine kinase-deficient mutant of equine herpesvirus 4 and in vitro susceptibility of the virus to antiviral agents. Antivir. Res. 85, 389–395. https://doi.org/10.1016/j.antiviral.2009.11.007.

Barbić, L., Lojkić, I., Stevanović, V., Bedeković, T., Starešina, V., Lemo, N., Lojkić, M., Madić, J., 2012. Two outbreaks of neuropathogenic equine herpesvirus type 1 with breed-dependent clinical signs. Vet. Rec. 170https://doi.org/10.1136/vr.100150. (227–227).

Barrandeguy, M., Thiry, E., 2012. Equine coital exanthema and its potential economic implications for the equine industry. Vet. J. 191, 35–40. https://doi.org/10.1016/j.tvjl.2011.01.016.

Carmichael, R.J., Whitfield, C., Maxwell, L.K., 2013. Pharmacokinetics of ganciclovir and valganciclovir in the adult horse. J. Vet. Pharmacol. Ther. 36, 441–449. https://doi.org/10.1111/jvp.12029.

Chapman, N., Dobson, J., Wilson, S., Dahlof, B., Sever, P.S., Wedel, H., Poulter, N.R., on behalf of the Anglo-Scandinavian Cardiac Outcomes Trial Investigators, 2007. Effect of spironolactone on blood pressure in subjects with resistant hypertension. Hypertension 49, 839–845. https://doi.org/10.1161/01.HYP.0000259805.18468.8c.

Charretier, C., Saulnier, A., Benair, L., Armanet, C., Bassard, I., Daulon, S., Bernigaud, B., Rodrigues de Sousa, E., Gonthier, C., Zorn, E., Vetter, E., Saintpierre, C., Riou, P., Gaillac, D., 2018. Robust real-time cell analysis method for determining viral infectious titers during development of a viral vaccine production process. J. Virol. Methods 252, 57–64. https://doi.org/10.1016/j.jviromet.2017.11.002.

Cooper, M.A., 2006. Non-optical screening platforms: the next wave in label-free screening? Drug Discov. Today 11, 1068–1074. https://doi.org/10.1016/j.drudis.2006.10.001.

Davison, A.J., Eberle, R., Ehlers, B., Hayward, G.S., McGeoch, D.J., Minson, A.C., Pellett, P.E., Roizman, B., Studdert, M.J., Thiry, E., 2009. The order Herpesvirales. Arch. Virol. 154, 171–177. https://doi.org/10.1007/s00705-008-0278-4.

De Clercq, E., 2013. Antivirals: past, present and future. Biochem. Pharmacol. 85, 727–744. https://doi.org/10.1016/j.bcp.2012.12.011.

De Clercq, E., Li, G., 2016. Approved antiviral drugs over the past 50 years. Clin. Microbiol. Rev. 29, 695–747. https://doi.org/10.1128/CMR.00102-15.

Diallo, I.S., Hewitson, G., Wright, L., Rodwell, B.J., Corney, B.G., 2006. Detection of equine herpesvirus type 1 using a real-time polymerase chain reaction. J. Virol. Methods 131, 92–98. https://doi.org/10.1016/j.jviromet.2005.07.010.

Diallo, I.S., Hewitson, G., Wright, L.L., Kelly, M.A., Rodwell, B.J., Corney, B.G., 2007. Multiplex real-time PCR for the detection and differentiation of equid herpesvirus 1 (EHV-1) and equid herpesvirus 4 (EHV-4). Vet. Microbiol. 123, 93–103. https://doi.org/10.1016/j.vetmic.2007.02.004.

Fang, Y., Ye, P., Wang, X., Xu, X., Reisen, W., 2011. Real-time monitoring of flavivirus induced cytopathogenesis using cell electric impedance technology. J. Virol. Methods 173, 251–258. https://doi.org/10.1016/j.jviromet.2011.02.013.

Friday, P.A., Scarratt, W.K., Elvinger, F., Timoney, P.J., Bonda, A., 2000. Ataxia and paresis with equine herpesvirus type 1 infection in a herd of riding school horses. J. Vet. Intern. Med. 14, 197–201.

Garre, B., Gryspeerdt, A., Croubels, S., De Backer, P., Nauwynck, H., 2009. Evaluation of orally administered valacyclovir in experimentally EHV1-infected ponies. Vet. Microbiol. 135, 214–221. https://doi.org/10.1016/j.vetmic.2008.09.062.

Garre, B., Vandermeulen, K., Nugent, J., Neyts, J., Croubels, S., Debacker, P., Nauwynck, H., 2007. In vitro susceptibility of six isolates of equine herpesvirus 1 to acyclovir, ganciclovir, cidofovir, adefovir, PMEDAP and foscarnet. Vet. Microbiol. 122, 43–51. https://doi.org/10.1016/j.vetmic.2007.01.004.

Giaever, I., Keese, C.R., 1993. A morphological biosenser for mammalian cells. Nature 366, 591–592.

Giaever, I., Keese, C.R., 1984. Monitoring fibroblast behavior in tissue culture with an applied electric field. Proc. Natl. Acad. Sci. 81, 3761–3764.

Goehring, L.S., Winden, S.C., Maanen, C. van, Oldruitenborgh-Oosterbaan, M.M.S., 2006. Equine herpesvirus type 1-associated myeloencephalopathy in the Netherlands: a four-year retrospective study (1999–2003). J. Vet. Intern. Med. 20, 601–607.

Golke, A., Cymerys, J., Słońska, A., Dzieciątkowski, T., Chmielewska, A., Tucholska, A., Bańbura, M., 2012. The xCELLigence system for real-time and label-free analysis of neuronal and dermal cell response to Equine Herpesvirus type 1 infection. Pol. J. Vet. Sci. 15. https://doi.org/10.2478/v10181-011-0126-4.

Goodman, L., Wagner, B., Flaminio, M., Sussman, K., Metzger, S., Holland, R., Osterrieder, N., 2006. Comparison of the efficacy of inactivated combination and modified-live virus vaccines against challenge infection with neuropathogenic equine herpesvirus type 1 (EHV-1). Vaccine 24, 3636–3645. https://doi.org/10.1016/j.vaccine.2006.01.062.

Henninger, R.W., Reed, S.M., Saville, W.J., Allen, G.P., Hass, G.F., Kohn, C.W., Sofaly, C., 2007. Outbreak of neurologic disease caused by equine herpesvirus-1 at a university equestrian center. J. Vet. Intern. Med. 21, 157–165.

Hue, E.S., Fortier, C.I., Laurent, A.M., Quesnelle, Y.F., Fortier, G.D., Legrand, L.J., Pronost, S.L., 2016. Development and validation of a quantitative PCR method for equid herpesvirus-2 diagnostics in respiratory fluids. J. Vis. Exp. https://doi.org/10.3791/53672.

Kydd, J.H., Slater, J., Osterrieder, N., Lunn, D.P., Antczak, D.F., Azab, W., Balasuriya, U., Barnett, C., Brosnahan, M., Cook, C., Damiani, A., Elton, D., Frampton, A., Gilkerson, J., Goehring, L., Horohov, D., Maxwell, L., Minke, J., Morley, P., Nauwynck, H., Newton, R., Perkins, G., Pusterla, N., Soboll-Hussey, G., Traub-Dargatz, J., Townsend, H., Van de walle, G.R., Wagner, B., 2012. Third international havemeyer workshop on equine herpesvirus type 1: EHV-1 havemeyer workshop report. Equine Vet. J. 44, 513–517. https://doi.org/10.1111/j.2042-3306.2012.00604.x.

Lacombe, B., Morel, M., Margottin-Goguet, F., Ramirez, B.C., 2016. Specific inhibition of HIV infection by the action of spironolactone in T cells. J. Virol. 90, 10972–10980. https://doi.org/10.1128/JVI.01722-16.

Léon, A., Fortier, G., Fortier, C., Freymuth, F., Tapprest, J., Leclercq, R., Pronost, S., 2008. Detection of equine herpesviruses in aborted foetuses by consensus PCR. Vet. Microbiol. 126, 20–29. https://doi.org/10.1016/j.vetmic.2007.06.019.

Limame, R., Wouters, A., Pauwels, B., Fransen, E., Peeters, M., Lardon, F., De Wever, O., Pauwels, P., 2012. Comparative analysis of dynamic cell viability, migration and invasion assessments by novel real-time technology and classic endpoint assays. PLoS One 7, e46536. https://doi.org/10.1371/journal.pone.0046536.

Lucas-Hourani, M., Munier-Lehmann, H., Helynck, O., Komarova, A., Desprès, P., Tangy, F., Vidalain, P.-O., 2014. High-throughput screening for broad-spectrum chemical inhibitors of RNA viruses. J. Vis. Exp. https://doi.org/10.3791/51222.

Lunn, D.P., Davis-Poynter, N., Flaminio, M.J.B.F., Horohov, D.W., Osterrieder, K., Pusterla, N., Townsend, H.G.G., 2009. Equine herpesvirus-1 consensus statement. J. Vet. Intern. Med. 23, 450–461. https://doi.org/10.1111/j.1939-1676.2009.0304.x.

Marlina, S., Shu, M.-H., AbuBakar, S., Zandi, K., 2015. Development of a Real-Time Cell Analysing (RTCA) method as a fast and accurate screen for the selection of chikungunya virus replication inhibitors. Parasit. Vectors 8. https://doi.org/10.1186/s13071-015-1104-y.

Mori, E., Borges, A.S., Delfiol, D.J.Z., Oliveira Filho, J.P., de, Goncalves, R.C., Cagnini, D.Q., Lara, M., Cunha, E.M.S., Villalobos, E.M.C., Nassar, A.F.C., et al., 2011. First detection of the equine herpesvirus 1 neuropathogenic variant in Brazil. Rev. Sci. Tech. -OIE 30, 949.

Noah, J.W., Severson, W., Noah, D.L., Rasmussen, L., White, E.L., Jonsson, C.B., 2007. A cell-based luminescence assay is effective for high-throughput screening of potential influenza antivirals. Antivir. Res. 73, 50–59. https://doi.org/10.1016/j.antiviral.2006.07.006.

Nugent, J., Birch-Machin, I., Smith, K.C., Mumford, J.A., Swann, Z., Newton, J.R., Bowden, R.J., Allen, G.P., Davis-Poynter, N., 2006. Analysis of equid herpesvirus 1 strain variation reveals a point mutation of the DNA polymerase strongly associated with neuropathogenic versus nonneuropathogenic disease outbreaks. J. Virol. 80, 4047–4060. https://doi.org/10.1128/JVI.80.8.4047-4060.2006.

Paillot, R., Case, R., Ross, J., Newton, R., Nugent, J., 2008. Equine herpes virus-1: virus, immunity and vaccines. Open Vet. Sci. J. 2.

Pan, T., Huang, B., Zhang, W., Gabos, S., Huang, D.Y., Devendran, V., 2013. Cytotoxicity assessment based on the AUC50 using multi-concentration time-dependent cellular response curves. Anal. Chim. Acta 764, 44–52. https://doi.org/10.1016/j.aca.2012.12.047.

Patel, J.R., Heldens, J., 2005. Equine herpesviruses 1 (EHV-1) and 4 (EHV-4) – epidemiology, disease and immunoprophylaxis: a brief review. Vet. J. 170, 14–23. https://doi.org/10.1016/j.tvjl.2004.04.018.

Pennington, M.R., Van de Walle, G.R., 2017. Electric cell-substrate impedance sensing to monitor viral growth and study cellular responses to infection with alphaherpesviruses in real time. mSphere 2, e00039–17. https://doi.org/10.1128/mSphere.00039-17.

Piret, J., Goyette, N., Boivin, G., 2016. Novel method based on real-time cell analysis for drug susceptibility testing of herpes simplex virus and human cytomegalovirus. J. Clin. Microbiol. 54, 2120–2127. https://doi.org/10.1128/JCM.03274-15.

Pitt, B., Perez, A., 1999. The effect of spironolactone on morbidity and mortality in patients with severe heart failure. N. Engl. J. Med. 9.

Pronost, S., Legrand, L., Pitel, P.-H., Wegge, B., Lissens, J., Freymuth, F., Richard, E., Fortier, G., 2012. Outbreak of equine herpesvirus myeloencephalopathy in France: a clinical and molecular investigation: outbreak of EHV-1 myeloencephalopathy. Transbound. Emerg. Dis. 59, 256–263. https://doi.org/10.1111/j.1865-1682.2011.01263.x.

Pronost, S., Léon, A., Legrand, L., Fortier, C., Miszczak, F., Freymuth, F., Fortier, G., 2010. Neuropathogenic and non-neuropathogenic variants of equine herpesvirus 1 in France. Vet. Microbiol. 145, 329–333. https://doi.org/10.1016/j.vetmic.2010.03.031.

Pusterla, N., Hussey, G.S., 2014. Equine herpesvirus 1 myeloencephalopathy. Vet. Clin. North Am. Equine Pract. 30, 489–506. https://doi.org/10.1016/j.cveq.2014.08.006.

Scrochi, M., Zanuzzi, C., Fuentealba, N., Nishida, F., Bravi, M., Pacheco, M., Sguazza, G., Gimeno, E., Portiansky, E., Muglia, C., Galosi, C., Barbeito, C., 2017. Investigation of apoptosis in cultured cells infected with equine herpesvirus 1. Biotech. Histochem. 1–9. https://doi.org/10.1080/10520295.2017.1359749.

Solly, K., Wang, X., Xu, X., Strulovici, B., Zheng, W., 2004. Application of real-time cell electronic sensing (RT-CES) technology to cell-based assays. Assay Drug Dev. Technol. 2, 363–372.

Spiegel, M., 1993. Real-time and label-free monitoring of virus-mediated cytopathogenicity. Nature 366.

Sudo, K., Konno, K., Yokota, T., Shigeta, S., 1995. A screening system for antiviral compounds against herpes simplex virus type 1 using the MTT method with L929 cells. Tohoku J. Exp. Med. 176, 163–171.

Teng, Z., Kuang, X., Wang, J., Zhang, X., 2013. Real-time cell analysis – a new method for dynamic, quantitative measurement of infectious viruses and antiserum neutralizing activity. J. Virol. Methods 193, 364–370. https://doi.org/10.1016/j.jviromet.2013.06.034.

Tian, D., Zhang, W., He, J., Liu, Y., Song, Z., Zhou, Z., Zheng, M., Hu, Y., 2012. Novel, real-time cell analysis for measuring viral cytopathogenesis and the efficacy of neutralizing antibodies to the 2009 influenza A (H1N1) virus. PLoS One 7, e31965. https://doi.org/10.1371/journal.pone.0031965.

Traub-Dargatz, J.L., Pelzel-McCluskey, A.M., Creekmore, L.H., Geiser-Novotny, S., Kasari, T.R., Wiedenheft, A.M., Bush, E.J., Bjork, K.E., 2013. Case-control study of a multistate equine herpesvirus myeloencephalopathy outbreak. J. Vet. Intern. Med. 27, 339–346. https://doi.org/10.1111/jvim.12051.

Trivedi, M.K., Shinkai, K., Murase, J.E., 2017. A Review of hormone-based therapies to treat adult acne vulgaris in women. Int. J. Women's. Dermatol. 3, 44–52. https://doi.org/10.1016/j.ijwd.2017.02.018.

Turowska, A., Pajak, B., Godlewski, M.M., Dzieciątkowski, T., Chmielewska, A., Tucholska, A., Banbura, M., 2010. Opposite effects of two different strains of equine herpesvirus 1 infection on cytoskeleton composition in equine dermal ED and African green monkey kidney Vero cell lines: application of scanning cytometry and confocal-microscopy-based image analysis in a quantitative study. Arch. Virol. 155, 733–743. https://doi.org/10.1007/s00705-010-0622-3.

Verma, D., Thompson, J., Swaminathan, S., 2016. Spironolactone blocks Epstein–Barr virus production by inhibiting EBV SM protein function. Proc. Natl. Acad. Sci. 113, 3609–3614.

Vissani, M.A., Thiry, E., Dal Pozzo, F., Barrandeguy, M., 2016. Antiviral agents against equid alphaherpesviruses: current status and perspectives. Vet. J. 207, 38–44. https://doi.org/10.1016/j.tvjl.2015.06.010.

Vissani, M.A., Zabal, O., Tordoya, M.S., Parreño, V., Thiry, E., Barrandeguy, M., 2018. In vitro comparison of acyclovir, ganciclovir and cidofovir against equid alphaherpesvirus 3 and evaluation of their efficacy against six field isolates. Rev. Argent. Microbiol. https://doi.org/10.1016/j.ram.2018.01.003.

Witkowski, P.T., Schuenadel, L., Wiethaus, J., Bourquain, D.R., Kurth, A., Nitsche, A., 2010. Cellular impedance measurement as a new tool for poxvirus titration, antibody neutralization testing and evaluation of antiviral substances. Biochem. Biophys. Res. Commun. 401, 37–41. https://doi.org/10.1016/j.bbrc.2010.09.003.

Zhang, J.-H., Chung, T.D.Y., Oldenburg Kevin, R., 1999. A simple statistical parameter for use in evaluation and validation of high throughput screening assays. J. Biomol. Screen. 4, 67–73.